

Coupling of the Intraseasonal Oscillation with the Tropical Cyclone in the Western North Pacific during the 2004 Typhoon Season

Huang-Hsiung Hsu, An-Kai Lo, Ching-Hui Hung, Wen-Shung Kau and Chun-Chieh Wu

Department of Atmospheric Sciences, National Taiwan University, Taipei, Taiwan
hsu@atmos1.as.ntu.edu.tw

Yun-Lan Chen

Weather Forecast Center, Central Weather Bureau, Taipei, Taiwan

A strong in-phase relationship between the intraseasonal oscillation (ISO) and the tropical cyclone (TC) was observed in the tropical western North Pacific from June through October 2004. The ISO, which is characterized by the fluctuations in the East Asian monsoon trough and the Pacific subtropical anticyclone, modulated the TC activity and led to the spatial and temporal clustering of TCs during its cyclonic phase. This clustering of strong TC vortices contributed significant positive vorticity during the cyclonic phase of the ISO and therefore enlarged the intraseasonal variance of 850 hPa vorticity. This result indicates that a significant percentage (larger than 50%) of observed intraseasonal variance along the clustered TC tracks in the tropical western North Pacific came from TCs. Numerical simulation confirmed that the presence and enhancement of TCs in the models enlarged the simulated intraseasonal variance. This implies that the contribution of TCs has to be taken into account to correctly estimate and interpret the intraseasonal variability in the tropical western North Pacific.

1. Introduction

The tropical western North Pacific is an active region for the tropical cyclone (TC) and the intraseasonal oscillation (ISO) in the northern summer (e.g. Lau and Chan, 1986; Wang and Rui, 1990; Elsberry, 2004; Hsu, 2005). Many studies have revealed the modulation effect of the ISO on the TC activity in this region (e.g. Nakazawa, 1986; Heta, 1990; Liebmann, *et al.*, 1994; Maloney and Dickinson, 2003). According to these studies, TCs tend to cluster in the westerly and positive vorticity phase of the ISO in the lower troposphere. Under the circumstances, one would wonder whether the clustering

of strong TC vortices may in turn increase the overall amplitude of positive vorticity in this phase, and therefore increase the intraseasonal variance (ISV) of vorticity. If this effect is in action, the ISV may not result entirely from the ISO itself. Instead, part of the variance may come from the clustered TC activity. This possibility has been explored and confirmed by Hsu *et al.* (2008), using the European Centre for Medium-range Weather Forecast reanalysis (ERA40, 1958–2002). This new finding suggests that the TC contribution must be considered to obtain a better understanding of the intraseasonal variability in the tropical western North Pacific.

The typhoon season (defined as June–October, JJASO) of 2004 was a unique season in the western North Pacific, in terms of the strong TC and ISO activity, and the in-phase relationship between the two. The most significant phenomenon was the record-breaking number (10) of typhoon landfalls in Japan. Another interesting feature was the temporal clustering, on the intraseasonal time scale, of the tropical cyclone genesis during the summer and early autumn. It was this strong in-phase relationship that led to the record-breaking typhoon landfalls in Japan, because the clustering effect of the ISO on TC resulted in the tendency for the typhoons to move along similar tracks (Nakazawa, 2006). In view of this close relationship between the TC and the ISO, this unique season enables an excellent case study of the coupling of the ISO and the TC. It is the goal of this study to explore the relationship between the TC and the ISO in this particular season, and to evaluate the contribution of the TC to the ISV.

In this study, an unconventional approach applied by Hsu *et al.* (2008) was employed in removing TCs from the global analysis. The potential contribution of TCs was estimated, which was defined as the variance difference between the original and TC-removed vorticity fields at 850 hPa. Numerical experiments based on a regional model and a general circulation model (GCM), with/without TCs and with enhanced TCs, were also carried out. Since similar results were obtained in GCM and regional model simulations, only the GCM results will be shown here for the sake of brevity. The approaches adopted in this study were designed to shed light on the TC contribution to the ISV along the TC tracks. Our results indicate that the differences in variance (i.e. the effect of TCs on the ISV) are large enough to be of concern on the intraseasonal time scale.

The arrangement of this article is as follows. Section 2 describes the data and methodology. ISO modulation on TCs is presented in Sec. 3,

and the TCs' potential contribution to the ISV is reported in Sec. 4. Simulation results and conclusions are presented in Secs. 5 and 6, respectively.

2. Data and Methodology

The wind and mean sea level pressure (MSLP) data used in this study were retrieved from National Centers for Environmental Prediction (NCEP) Reanalysis I on a 2.5°-by-2.5° grid, while the TC statistics and best-track data were obtained from the Japanese Meteorological Agency (JMA) and the Joint Typhoon Warning Center (JTWC), respectively. A 32–76-day Butterworth band-pass filter (Kaylor, 1977) was applied to NCEP Reanalysis I to extract the intraseasonal fluctuations from the daily mean vorticity. The reason for the choice of the 32–76-day band will be presented in a later section. To reduce the end effect of the Butterworth filter, only data from 16 June to 15 October were used to calculate the ISV.

In reality, due to the possible nonlinear TC–climate interaction, it is impossible to exactly quantify the TC contribution. This essentially holds good for all studies involving multiple temporal and spatial scales. Despite this concern, temporal and spatial filtering has often been used to decompose a total field into perturbation and mean flow, or even into several subfields of distinct temporal or spatial scales. This linear-thinking approach has proved useful in providing important insights into climate processes, such as the wave–mean flow interaction. In order to evaluate the possible TC contribution to the ISV in the western North Pacific during the 2004 typhoon season, a spatial filtering approach was taken to remove the TC vortices from the 850 hPa vorticity. This filtering procedure is similar to the decomposition of the total field into perturbation and background flow, but is performed in a more sophisticated manner. The potential contribution of TCs to the ISV was

estimated by calculating the difference between the ISV of the original and the TC-removed vorticity at 850 hPa.

Removal of TCs from the analysis data has been a common practice in typhoon and hurricane simulation and forecasting. The procedure, which has been used in the Geophysical Fluid Dynamics Laboratory (GFDL) hurricane prediction system (Kurihara *et al.*, 1993, 1995) and in typhoon simulations (Wu *et al.*, 2002) for enhancing the representation of the environmental field in the initial condition, has proved effective in improving the overall TC track forecast. Following the procedure proposed by Kurihara *et al.* (1993, 1995), the four-time daily 850 hPa winds associated with each TC, based on the JTWC best track, were subtracted from the 850 hPa wind field during the typhoon season.

The basic procedure, demonstrated in Fig. 1, is briefly described as follows. [See Kurihara *et al.* (1993, 1995) for details.] The zonal and meridional winds were individually separated into basic and disturbance fields using a smoothing operator. The winds associated with a TC were isolated in the filter domain, which

defines the extent of a TC in the global analysis, and subtracted from the disturbance field to create a non-TC component. In the procedure, 1200 km is specified as the radius of the filter domain. This does not mean that everything in the domain is identified as the TC component. It is simply the longest distance for the procedure to automatically search the effective radius of a TC in 24 directions (for every 15°) surrounding the TC center. When the radius of a TC, e.g. 500 km, is identified in a particular direction, the searching stops, and only the TC winds within the radius are subtracted. The reason for choosing a larger domain is to avoid missing the TC circulation in a TC (or typhoon) that has a large radius, and which would lead to underestimation of the TC circulation. After removing the TC component from the disturbance field, the non-TC component was added to the basic field to form the environmental flow, which is the TC-removed wind field in this study. The environmental flow outside the filter domain is identical to the original global analysis. The original and TC-removed vorticity fields were calculated based on the corresponding wind fields.

Hsu *et al.* (2008) demonstrated that the TC-removing procedure is able to correctly separate the TC and environmental components. One example is shown in Fig. 2 — three typhoons appeared simultaneously in the western North Pacific on 28 August 2004. They appear as three isolated vortices (i.e. the TC component) in Fig. 2(b), while the environmental flow (background flow plus non-TC component) is clearly characterized by the zonally elongated monsoon trough [Fig. 2(c)] across the South China Sea and the Philippine Sea. This result, as in many other cases, indicates that the TC removal procedure removes mainly the TC vortex and accurately retains the large-scale circulation, along with the climate variability contributed by the large-scale fluctuations.

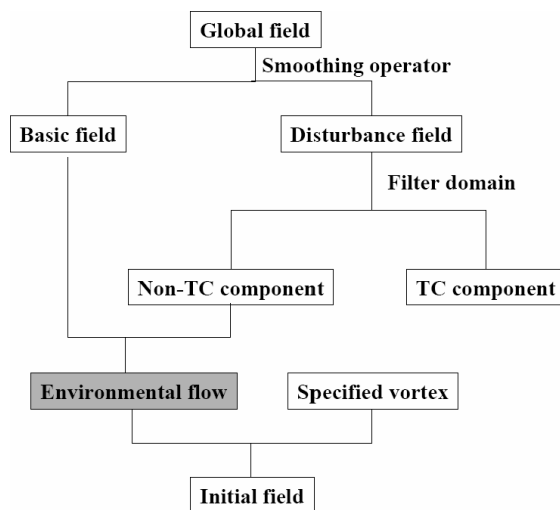


Figure 1. Flow chart of the TC removal procedure.

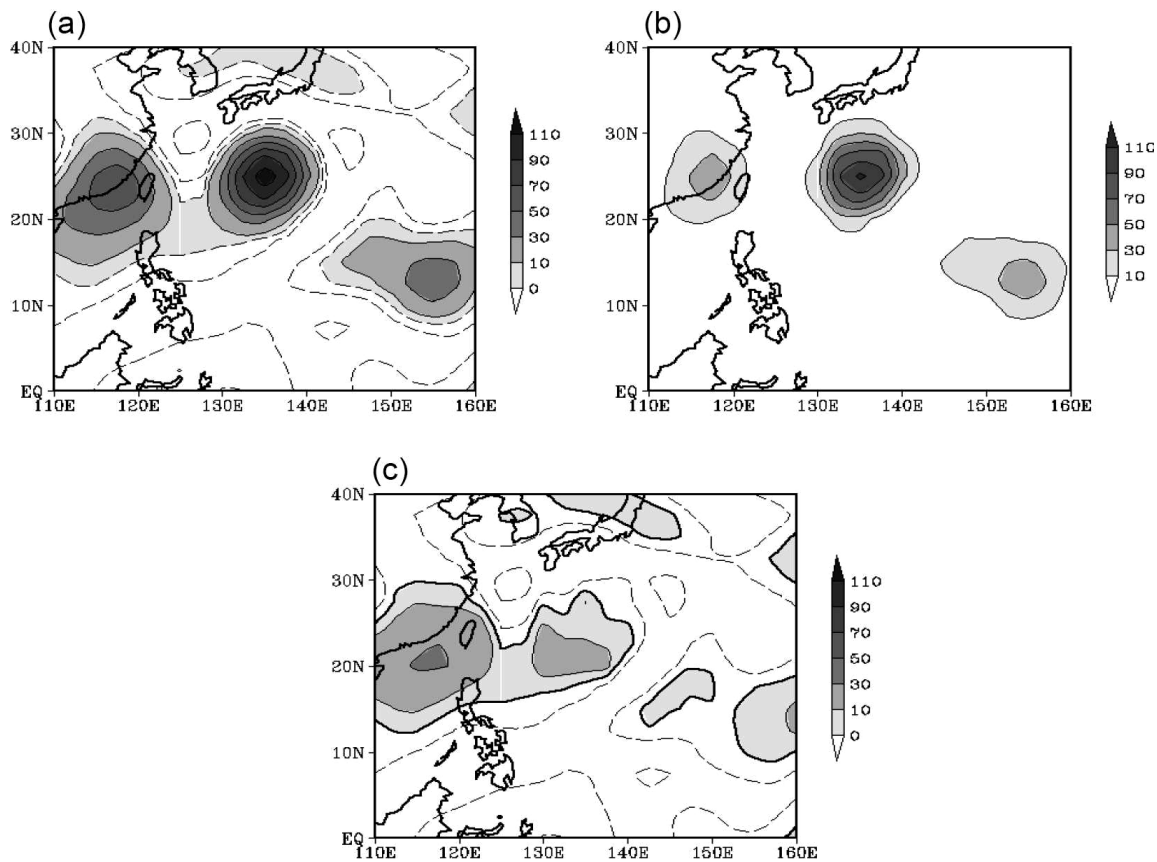


Figure 2. 850 hPa vorticity fields on 26 August 2004, when three typhoons were observed in the tropical western North Pacific: (a) total field, (b) TC and (c) environmental component. The unit for the contour is 10^{-6} s^{-1} .

One potential problem in removing TCs from the global analysis, such as NCEP Reanalysis I, is the possible mismatch between the JTWC TC track, which defines the center of a TC, and the position of the TC-corresponding vortex in NCEP Reanalysis I. This is partially attributed to the coarse resolution of the data set commonly used in climate study. The JTWC best track and NCEP Reanalysis I were examined, and a general consistency, although not an exact match, was found. The main goal of this study is to statistically assess the gross contribution of TCs to the climate variability in a large domain covering the entire tropical western North Pacific. A mismatch of a few degrees in latitude and longitude would not seriously affect the overall results. As will be

seen later, the removed vorticity is collocated nicely with the TC tracks. The possible mismatch does not seem to cause problems in this study. TCs may be presented differently in different global analyses or in different resolutions. Hsu *et al.* (2008), who compared the results derived from the European Centre for Medium-range Weather Forecast reanalysis and the NCEP reanalysis, and also between different spatial resolutions, demonstrated the general consistency between the analyses and the effectiveness of the TC-removing procedure adopted in this study. Their results suggest that the overall results presented here are not affected by different analyses and spatial resolutions, although certain quantitative differences may be found.

Another concern is the underrepresentation of the wind speed and vorticity of TCs in the global analysis. This is an existing problem, which cannot be solved in this study. The study's goal is to demonstrate how TCs contribute significantly to the ISV, based on presently available global analysis. The results should be viewed as the TC effect represented in currently available global analysis, which has been widely used to estimate the ISV. If the exact location and strength of TCs are represented in the global analysis, the actual contribution of TCs will likely be larger than what was found in this study.

3. ISO and TC

Based on the JMA statistics, there were 29 named TCs (including tropical storms and typhoons) in the western North Pacific during the 2004 typhoon season, slightly more than the climatological mean of 26.7. Most of the TCs in this period tended to appear in clusters quasi-periodically, as noted in previous studies

(e.g. Gray, 1979; Nakazawa, 2006). This clustering phenomenon is closely associated with the fluctuations of the monsoon trough and subtropical anticyclone (e.g. McBride, 1995; Harr and Elsberry, 1998; Elsberry, 2004). The tendency of TC occurrence in or near the East Asian (EA) monsoon trough was particularly evident in 2004. Climatologically, the movement of TCs can be roughly classified into two types: straight-moving track and recurving track. The former type of TC moves across the Philippine Sea in the northwest direction toward southern China and the Indochina peninsula, while the latter type recurves northeastward following a certain period of northwestward movement over the Philippine Sea. During the June–October period, the ratio between the straight-moving and the recurving track is about 1:1 for those TCs formed south of 20°N (Harr and Elsberry, 1998). However, most of the TCs in JJASO 2004 moved northwestward over the Philippine Sea, recurving northeastward when approaching the subtropics. This clustering phenomenon can be seen clearly in Fig. 3, which presents the

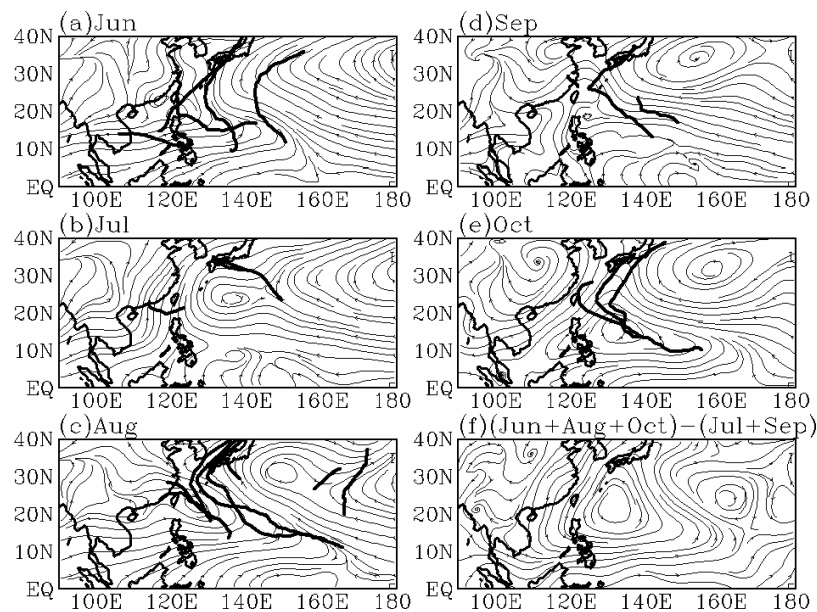


Figure 3. Monthly mean 850 hPa streamline and named TC tracks from (a) June to (e) October 2004, and (f) the difference between the June/August/October and July/September mean circulation at 850 hPa.

monthly-mean 850 hPa streamlines and the TC tracks for each month from June to October. Note that the recurving occurred most evidently in June, August, and October, when TCs were more active.

The EA monsoon trough extended southeastward from the Indochina peninsula to the Philippine Sea, and contracted westward intermittently from June to October. There were more-than-average numbers of tropical storms in June (5), August (8), and October (4), compared to the 1971–2000 climatological mean numbers of 1.7, 5.5, and 2.8, when the EA monsoon trough was active and extended further southeastward than normal. Fewer tropical storms occurred in July (2) and September (3), compared to the climatological mean numbers of 4.1 and 5.1, respectively, when the EA monsoon trough was weak and contracted westward. It is known that TCs tend to occur in or near the EA monsoon trough (e.g. Elsberry, 2004; Chen *et al.*, 2004). This relationship seems particularly evident in JJASO 2004. Most of the TCs also seemed inclined to move in a clockwise direction along the southern and western peripheries of the Pacific anticyclone. This movement pattern is similar to the recurve-south track identified by Harr and Elsberry (1998). It appears that the fluctuations of the EA monsoon trough and the Pacific anticyclone strongly modulated the TC activity in this particular season.

The intermittent occurrence of the eastward extension and westward contraction of the EA monsoon trough in JJASO 2004 was associated with strong ISO activity. To identify this intraseasonal signal, an index was designed to represent the fluctuation in the EA monsoon trough. The index is defined as the MSLP averaged over the region (120°E–150°E, 10°N–20°N), where the extension and contraction of the EA monsoon trough is most evident (Fig. 3). Wavelet analysis (Torrence and Compo, 1998) on this daily index from April to December 2004 was performed to identify the dominant

periodicity. As shown in Fig. 4(a), large fluctuations are evident in the 32–76-day and 11–27-day bands throughout the period. The accumulated variance explained by the 32–76-day perturbations accounted for 54.5% of the total variance in JJASO 2004, while the 11–27-day period accounted for 29.3%. The 32–76-day ISO was apparently the major fluctuation to affect the EA monsoon trough. In view of its dominance in variance, the following discussion will focus on the 32–76-day ISO. To further reveal the uniqueness of the this ISO in 2004, wavelet analysis was performed on the EA monsoon trough index during the June–October season from 1951 to 2004 annually. The result shown in Fig. 4(b) reveals that the 32–76-day variance in 2004 was the largest from 1951 to 2004, indicating the strongest intraseasonal fluctuation of the EA monsoon trough in this 54-year period. This variance (almost 3 hPa²) is much larger than the second-largest variance (about 2 hPa²) occurring in the 1979 summer, which was known as a summer of strong ISO activity (Lorenc, 1984). The JJASO of 2004 was obviously a unique season for the 32–76-day ISO. The reason for this large ISV is not clear and will be explored in other studies.

Spatial distribution of the 32–76-day ISV of MSLP in JJASO 2004, shown in Fig. 5(a), exhibits two centers of maximum variance: one over the Philippine Sea, and in the extratropical North Pacific. A comparison between Fig. 3 and Fig. 5(a) indicates that the large variances over the Philippine Sea and the extratropical North Pacific were associated with the movement and fluctuation of the EA monsoon trough and the Pacific anticyclone during the season, respectively. The shading shown in Fig. 5(a) indicates the percentile of the 32–76-day variance in JJASO 2004 at every point, compared to all JJASO variances in the 54-year period. The area exceeding the 90th percentile covers most of East Asia and the western North Pacific, while small variance appears in the Indochina peninsula, the South China Sea, and the equatorial

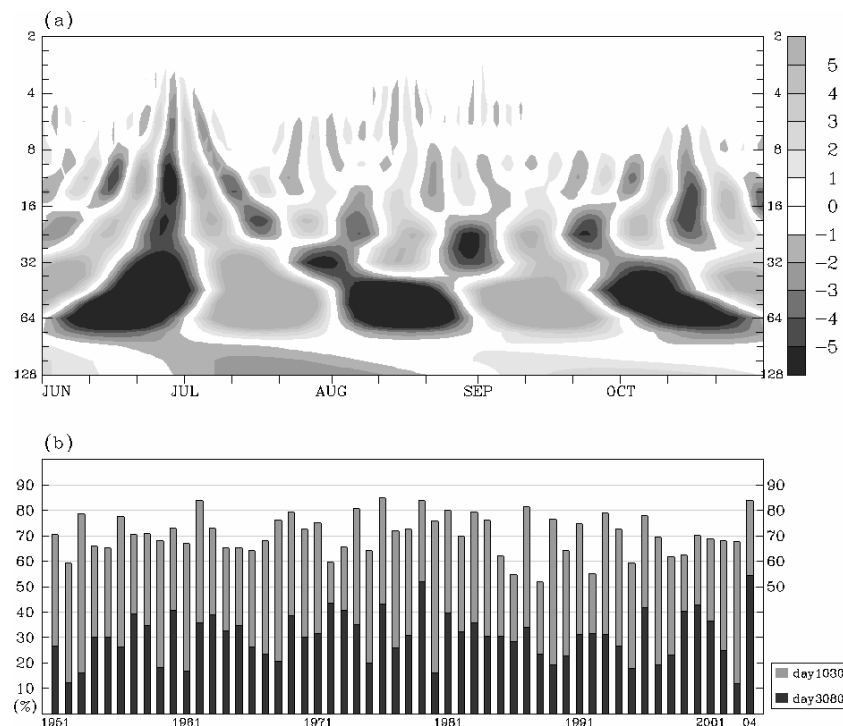


Figure 4. (a) Wavelet coefficients for the EA monsoon trough index (see text), (b) the percentages of the index variance explained by the 11–27-day (blue bar) and 32–76-day (red bar) bands for the 54 years from 1951 to 2004. The vertical axis in (a) and (b) denotes the period in days and percentage, respectively, while the horizontal axis in (a) and (b) denotes dates from June to October 2004 and years from 1951 to 2004, respectively.

western Pacific. The area chosen to construct the index is well inside the 95% region. The index designed to reflect the large fluctuation in the monsoon trough appears adequately chosen. The distribution shown in Fig. 5(a) indicates that the unusually active ISO in JJASO 2004 occurred not only in the EA monsoon trough but also in other EA summer monsoon regions (e.g. eastern China, Taiwan, Japan, and Korea).

The spatial distribution of the 32–76-day OLR variance is shown in Fig. 5(b) to reveal the ISV in convection. A large variance area exceeding the 90th percentile is observed in the tropical western North Pacific, located to the southeast of its MSLP counterpart. A large variance and high percentile area is also found near Japan, reflecting the large number of typhoons affecting Japan and possibly the

clustering effect of the ISO on the typhoon activity. These results indicate that the anomalously active intraseasonal fluctuations existed in both the circulation and convection fields during JJASO 2004.

The strong ISV of the EA monsoon trough and the Pacific anticyclone apparently resulted in the spatial and temporal clustering of TCs. This close relationship is shown in Fig. 6, which presents the composite of MSLP and the TC tracks during three cyclonic phase months (June, August, and October — upper panel) and two anticyclonic phase months (July and September — lower panel) appearing intermittently as shown in Fig. 3, respectively. The majority of TCs during JJASO occurred in the cyclonic phase, as indicated by the negative MSLP anomaly, and tended to take a recurving track, while only a few appeared in the anticyclonic

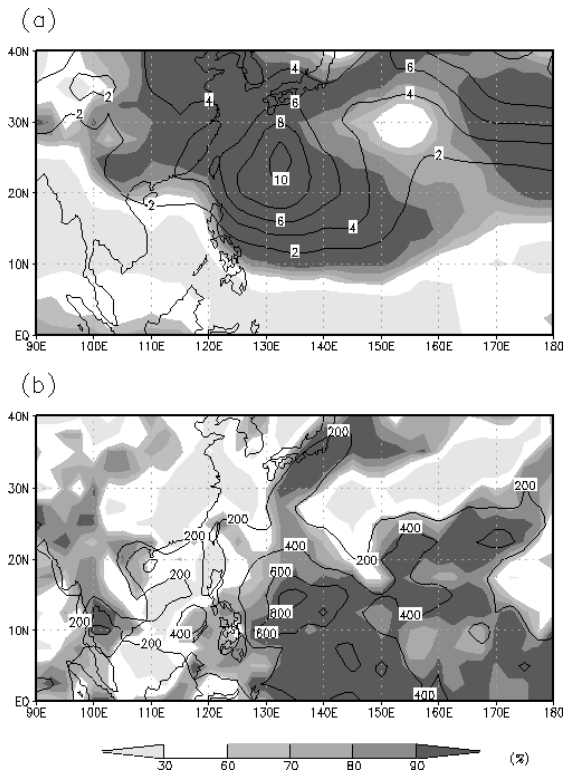


Figure 5. Spatial distribution of the 32–76-day filtered (a) MSLP and (b) OLR variance in JJASO 2004. The contour intervals are 2 hPa^2 and $200 (\text{W/m}^2)^2$ for MSLP and OLR, respectively. Shading indicates the percentile of the 2004 variance in the 54-year period from 1951 to 2004.

phase in an environment of the positive MSLP anomaly.

The close ISO–TC relationship is further demonstrated in Fig. 7, which presents the 32–76-day fluctuation in the MSLP averaged between 120°E and 150°E , and the latitudinal positions of TSs that happened to be situated in this longitudinal band. A sequence of the 32–76-day ISO propagated northward from 10°N to 30°N regularly from June to October. Evidently, many more TSs appeared in the negative phase than in the positive phase of the ISO and moved northward in an anomalous low-pressure environment. As found in many previous studies, the genesis and track of the TCs in the tropical western North Pacific during JJASO 2004 were strongly modulated by the intermittent

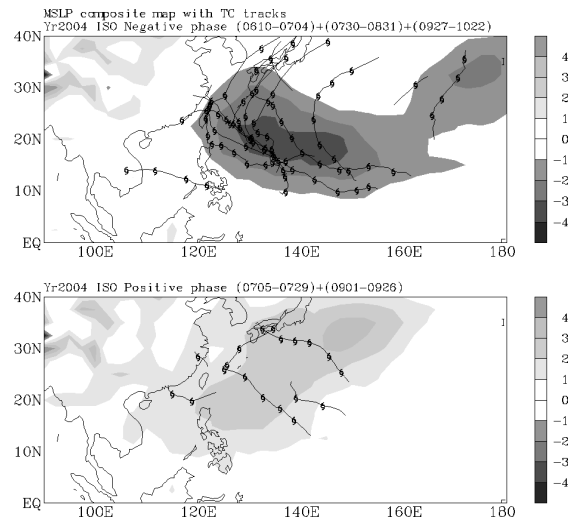


Figure 6. Composites of MSLP for (upper) three cyclonic phases and (lower) two anticyclonic phases. The TC tracks during these two phases are also marked. Periods chosen for composites are shown at the top of each figure.

extension and retraction of the monsoon trough, which was in turn affected by the unusually strong ISO.

4. TC Contribution to the ISV

The potential contribution of TCs to the ISV was estimated by calculating the difference between the ISV was the original and the TC-removed vorticity at 850 hPa. As demonstrated in Fig. 2 and Hsu *et al.* (2008), the Kurihara scheme cleanly separates TCs from the background large-scale circulation. The variance contributed by TCs and large-scale circulation are also well separated. The original 32–76-day variance of 850 hPa vorticity presented in Fig. 8(a) reveals two major ISV regions along the TC tracks: one elongated region in the Philippine Sea and the other south of Japan. The former corresponds to the northwestward TC tracks, while the latter corresponds to the recurving TC tracks toward Japan. After the removal of TCs, the variance in these two regions reduced dramatically, as shown in Fig. 8(b), while the variance outside these two regions

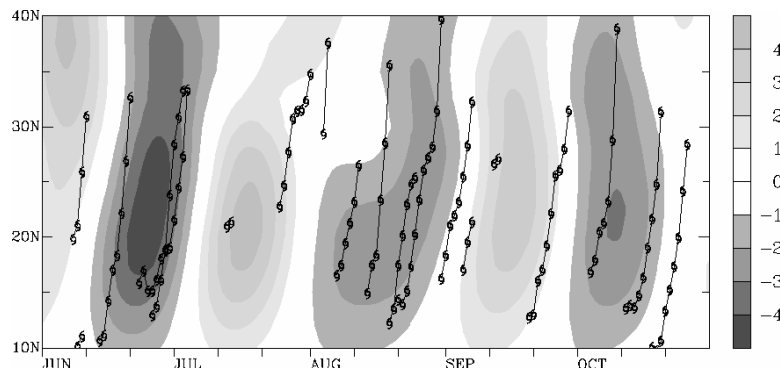


Figure 7. Hovmöller diagrams for the 32–76-day filtered MSLP averaged between 120°E and 150°E. The contour interval is 1 hPa. The latitudinal positions of the TCs that happened to be in 120°E–150°E are marked.

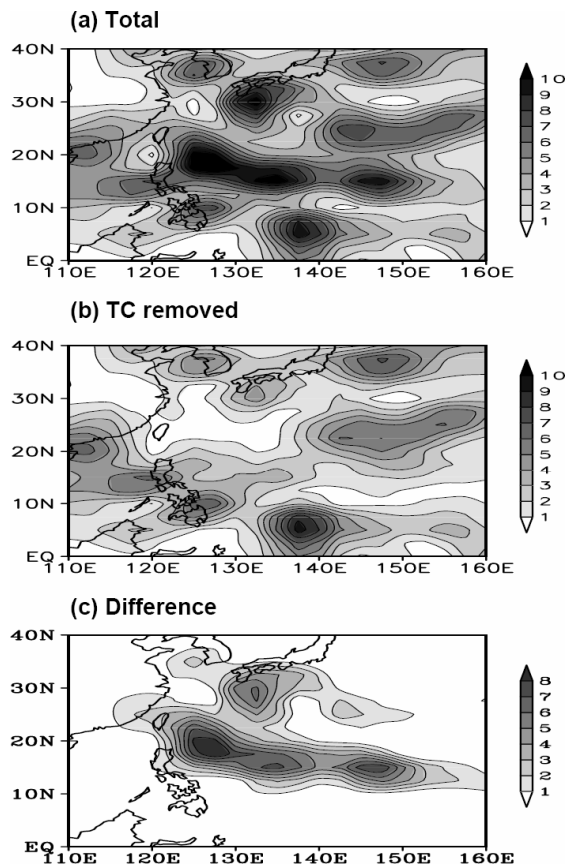


Figure 8. Intraseasonal (32–76-day) variance of the (a) original and (b) TC-removed 850 hPa vorticity. The difference between (a) and (b) is shown in (c). Only values greater than $1 \times 10^{-11} \text{ s}^{-2}$ are plotted.

remained almost unchanged. The variance difference shown in Fig. 8(c) indicates that the amount of the variance contributed by the clustered TCs can be as large as 50–80%.

To illustrate how the TCs contribute to the ISV in the statistical sense, the time series of the original and TC-removed 850 hPa vorticity was averaged over 125°E–140°E, 15°N–22.5°N, where the maximum variance is observed, and the difference between the two is shown in Fig. 9(a). Positive vorticity peaks occurred in groups in June, August, and October, indicating the clustering of TCs, while weak negative vorticity was observed during the TC-inactive period (July and September). Removal of TCs apparently results in a significantly reduced amplitude of the positive vorticity peaks, but it has no effect on negative vorticity for an obvious reason. This leads to the overall enlargement of positive vorticity during the TC-active periods, which recurred on the intraseasonal time scale, and therefore the increased ISV for the whole JJASO season. For example, the ISV in the above region drops from $5.9 \times 10^{-11} \text{ s}^{-1}$ to $2.2 \times 10^{-11} \text{ s}^{-1}$ after the TC removal. This significant reduction can also be seen in the spectra of the area-averaged vorticity presented in Fig. 9(b). While the original and the TC-removed spectral density exhibit qualitatively

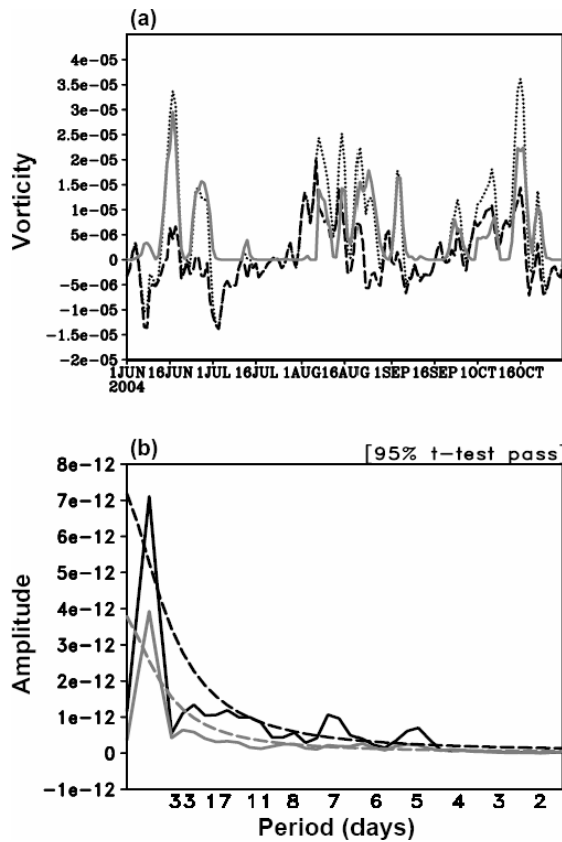


Figure 9. (a) Time series of the area-averaged 850 hPa vorticity over 125°E – 140°E , 15°N – 22.5°N from June to October 2004. The dotted and dashed lines represent the original and TC-removed vorticity fields, respectively, while the thick solid line represents the difference. (b) Spectra density of the original (dark solid line) and the TC-removed (light solid line) time series shown in (a). Dashed lines represent the 95% confidence limits. Fluctuations with periods longer than 120 days were removed before calculating the spectral density.

similar distribution in frequency, the intraseasonal peak (statistically significant at the 0.05 level) drops by about 50% in the TC-removed case. In addition, removal of TCs also results in a reduction of the seasonal mean vorticity. For example, the seasonal mean vorticity in the region chosen for Fig. 4(a) is $2.1 \times 10^{-5} \text{ s}^{-1}$ in the original vorticity but reduces to almost zero in the TC-removed vorticity. These results indicate that the presence of TCs in the tropical western North Pacific not only enlarges the ISV

but also increases the seasonal mean vorticity along the TC tracks. In a recent study, Hsu *et al.* (2008) demonstrated that the presence of TCs enhances not only the ISV but also the inter-annual variance.

In view of the large reduction in the ISV after the removal of TCs, one would wonder whether the propagation of the ISO is affected. Figure 10 presents the latitude-time Hovmöller diagram of the 850 hPa vorticity averaged between 120°E and 150°E , where the ISO exhibits obvious northward propagation. The original ISO exhibited two cycles of oscillation, with the largest amplitudes near 5°N and 15°N , and a node near 10°N [Fig. 10(a)]. In between the occurrence of maximum amplitudes, northward propagation from 5°N to 15°N was evident. After the removal of TCs, the amplitude of the vorticity weakens significantly between 10°N and 20°N , where TC tracks were located, while the pattern and amplitude at other latitudes are nearly unchanged [Fig. 10(b)]. The northward propagation from 5°N to 15°N , which is the major characteristic of the ISO in this region during the boreal summer, is still evident.

Since the TCs' effect on the ISO mainly occurred in the 10°N – 20°N latitudinal band, the longitude-time Hovmöller diagram of the 850 hPa vorticity averaged between 10°N and 20°N was examined. In Fig. 10(c), two cycles of the ISO with the maximum amplitude at various longitudes are evident. There are signs of westward propagation in the early half of summer, especially over 120°E – 140°E , and eastward propagation in the latter half of summer. After the removal of TCs, the amplitude of the ISO reduces significantly, while the pattern remains similar [Fig. 10(d)], although there are indications of weakened eastward propagation between 140°E and 155°E in the latter half of summer. Overall, the most significant effect of TCs on the ISO is the large reduction in the amplitude. In comparison, the TCs' effect on the phase and propagation of the ISO is minimal.

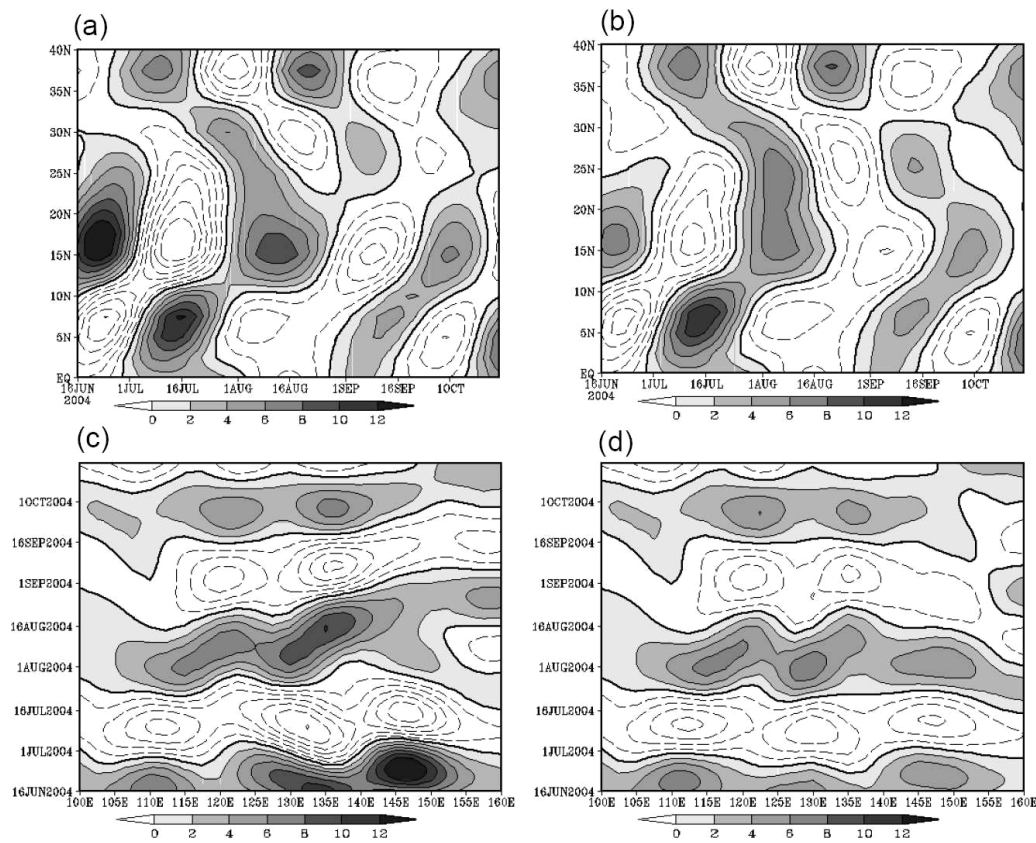


Figure 10. Hovmüller diagrams for the (upper left) original and (upper right) the TC-removed 32–76-day filtered 850 hPa vorticity averaged over 120°E – 150°E , and for the (lower left) original and the (lower right) TC-removed 32–76-day filtered 850 hPa vorticity averaged over 10°N – 20°N . The contour intervals are $3 \times 10^{-6} \text{ s}^{-1}$ and $2 \times 10^{-6} \text{ s}^{-1}$ for the upper panel and the lower panel, respectively.

5. Numerical Experiment

The empirical results presented above reveal the significant effect on the amplitude and variance of the ISO. This section presents numerical simulations performed to see whether similar effects could be realized in the numerical models. Two models were used in this study. The first was the Purdue regional model (PRM), which had been used for the study of various mesoscale phenomena (e.g. Sun *et al.*, 1991; Hsu and Sun, 1994; Sun and Chern, 1993) and climate simulation (e.g. Bosilovich and Sun, 1998, 1999; Hsu *et al.*, 2004; Sun *et al.*, 2004). The second one was the National Taiwan University's general circulation model (NTUGCM; Hsu *et al.*, 2001).

The resolution for the PRM was 60 km in the horizontal and 28 levels in the vertical. The model domain is 90°E – 160°E and 0 – 40°N , with a 15-point buffer zone on the lateral boundary. The ECMWF advanced analysis at 1.125° resolution was used as the initial condition and the lateral boundary condition. The latter was updated every 6 hours. The resolution for the NTUGCM was T42 in the horizontal and 13 levels in the vertical. The ECMWF basic analysis at 2.5° resolution was used as the initial condition.

Both models show a certain degree of ability to simulate TCs in the first few days. One example for the NTUGCM is shown in Fig. 11 for the forecast with initial condition at 00Z

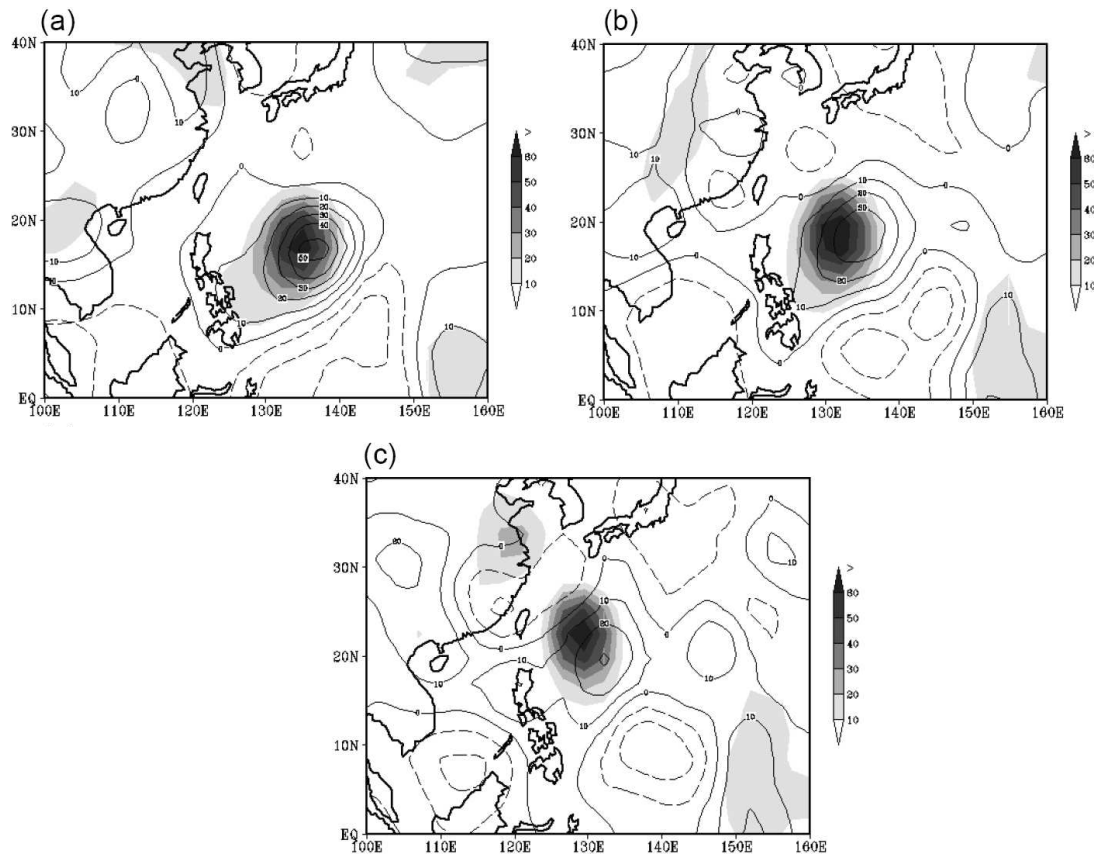


Figure 11. (a) 24-hour, (b) 48-hour, and (c) 72-hour hindcast of 850 hPa vorticity (contour) by the NTUGCM, initialized from 00Z 16 June 2004. The observed vorticity is plotted in shading.

16 June. The 24-hour hindcast [Fig. 11(a)] was able to simulate the location of TCs, although with a much weaker amplitude. The TC vortex looks larger and smoother because of the low resolution. In the 48-hour and 72-hour hindcasts [Figs. 11(b) and 11(c)], the simulated TC-like vortex is still evident, but lags behind the observed TC vortex. The 48-hour and 72-hour hindcasts generally show large track bias and smaller amplitudes.

It appears that both models are able to produce satisfactory simulation in the 24-hour hindcast. To evaluate the TCs' effect on the simulated ISV, different numerical experiments were performed. A series of 24-hour hindcasts were performed daily, using both models, from 1 June to 31 October 2004. They yielded a

dataset of the control experiment in JJASO, which was used for diagnostics like the real data. Three series of the NTUGCM experiment were performed. The first is a series of 24-hour hindcasts starting with the observed initial conditions. The second is the same as the first, except that TCs have been removed from the initial condition. The third is a 24-hour hindcast experiment, starting with the observed initial condition, in which the vorticity in the lower troposphere was artificially enhanced where the TCs are located. The vorticity was enhanced at the grid points, where the surface pressure was lower than 980 hPa and the 900 hPa/850 hPa/700 hPa mean vorticity was larger than 0.00005 s^{-1} . The vorticity at 900 hPa/850 hPa/700 hPa was multiplied by

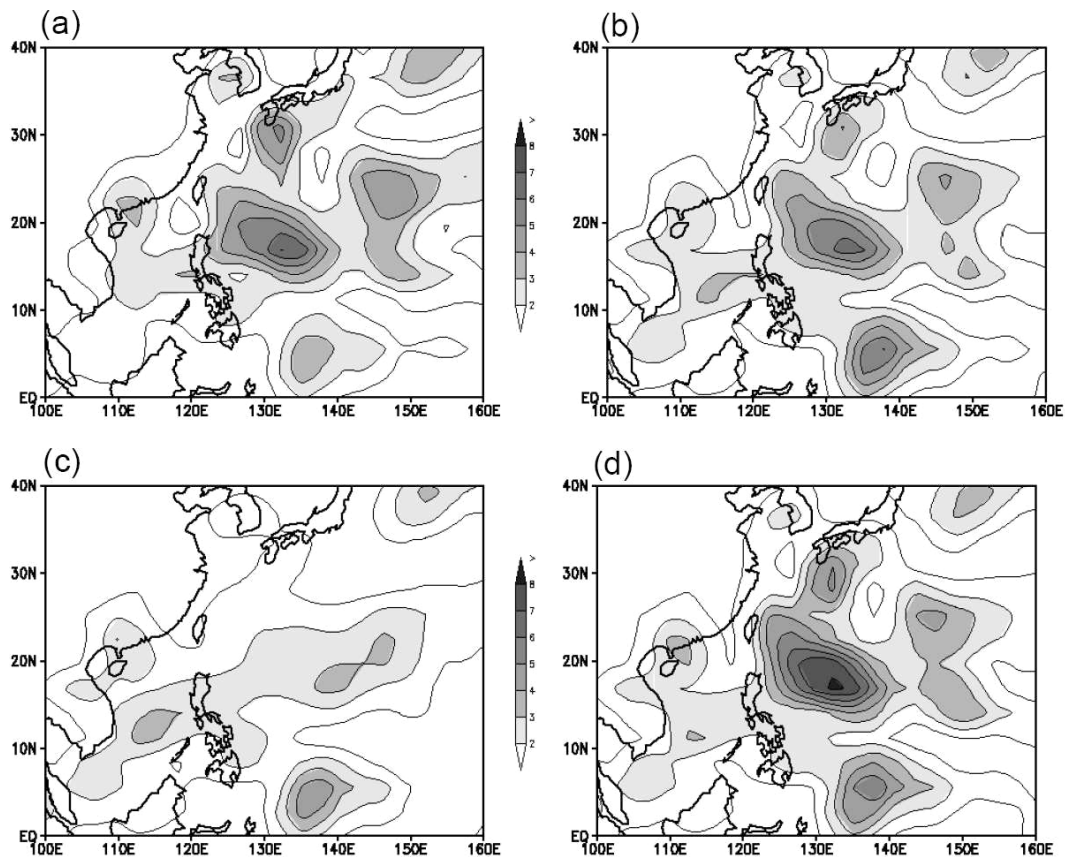


Figure 12. Variance of the 32–76-day filtered 850 hPa vorticity for (a) the observed and the (b) control, (c) TC-removed, and (d) vorticity-enhanced simulations using the NTUGCM. The contour interval is $0.5 \times 10^{-10} \text{ s}^{-2}$.

1.15/1.01875/1.00555, respectively. These three experiment series were performed daily from 1 June to 31 October, and the 32–76-day band-pass filter was applied to the three simulation datasets. Both the simulated and the observed ISV of the 850 hPa vorticity are shown in Fig. 12. The observed ISV, which is plotted at the NTUGCM spatial resolution, looks much smoother because of the low spatial resolution [2.5° by 2.5° ; Fig. 12(a)]. The control experiment [Fig. 12(b)] was able to reproduce a realistic spatial distribution of the ISV with a slightly weaker magnitude. In contrast, the TC-removed experiments [Fig. 12(c)] failed completely to simulate the maximum variance along the TC tracks. The vortex-enhanced experiments [Fig. 12(d)], on the contrary, not only

simulated well the ISV distribution but also enhanced the magnitude to the observed level. A comparison between the results obtained from the three experiment series indicates that the presence and enhancement of TC-like disturbance, although fluctuating at a much higher frequency, enhance the ISV.

A series of heating-enhanced hindcast experiments using the PRM were performed, by adding a prescribed heating profile to the simulated TC-like vortices. The heating profile mimics the Q1 profile (not shown), which was calculated from the reanalysis at those grid points where category-4 typhoons passed. The profile was characterized by the maximum heating at 600 hPa, and the decreasing linearly upward and downward. However, the heating

below 800 hPa was kept constant, to obtain better simulation. During the simulation, the heating was multiplied by 2 and held constant at the center of TC-like vortices, and exponentially decreased outward for 10 grid points. Since this was an idealized experiment, the prescribed heating is the same for all cases at all times, disregarding the different sizes and strengths of the vortices. The purpose was to artificially and significantly enhance the strength of the TC-like vortices in the model and, through a comparison with the controlled experiments, to evaluate whether the TCs can enhance the ISV in the simulation.

The 32–76-day band-pass filter was applied to the 850 hPa vorticity of the control and heating-enhanced hindcast experiments to extract the intraseasonal fluctuation. The control experiment was able to reproduce the overall distribution of the ISV, but the values are only about 1/3 of the observed variance. This is because the simulated TC-like vortices are weaker than the observed, and tend to weaken quickly. The simulated variance in the heating-enhanced experiments is raised to the equivalent level of the observed magnitude, while maintaining a realistic spatial distribution. This contrast indicates that the enhanced TC-like disturbance in the regional model also contributed to enhancing the ISV. The results of numerical experiments confirm the hypothesis, which was proposed based on the empirical results, that the presence of TCs in clusters can enhance the ISV.

6. Conclusions and Discussion

This study has revealed the strong ISO–TC in-phase relationship in the tropical western North Pacific during JJASO 2004. The repeated appearance of the ISO during JJASO resulted in the fluctuation of the EA monsoon trough and the Pacific anticyclone, which in turn modulated the TC activity and led to the spatial and temporal clustering of TCs. While TCs occurred in groups during the cyclonic phase of the ISO, the clustering of these strong TC vortices

significantly increased the overall amplitude of positive vorticity during the cyclonic phase of the ISO. On the contrary, the overall amplitude of negative vorticity during the anticyclonic phase of the ISO remained unaffected, because of poorly organized TC activity in the anticyclonic phase of the ISO. The ISV was therefore enlarged with the occurrence of TCs. This result reveals that a significant percentage (larger than 50%) of the observed ISV in the tropical western North Pacific was contributed by TCs along the clustered TC tracks. This large contribution, which has not been well recognized, was clearly present in the 2004 typhoon season and is likely to have occurred in other years as well. Hsu *et al.* (2008) reported similar results, based on a study using multiyear datasets. A series of 24-hour hindcast numerical experiments with various designs were performed to evaluate the effect of TC-like vortices on the simulated ISV. Results of both the regional model and the GCM indicated that the experiments with larger TC-like vortices produced a stronger ISV and better simulations in terms of both spatial distribution and magnitude. This finding is consistent with the conclusion inferred from the empirical results.

The extraordinarily strong ISV and its coupling with TCs have been clearly demonstrated. This unusual phenomenon apparently led to the record-breaking number of typhoon landfalls in Japan. However, what mechanism led to these unusual features (e.g. the largest ISV in 54 years, the strong coupling between ISO and TC, the location of strong ISV) is still unknown. One may suspect that the warm SST might have an effect on the ISO and TC since it was an El Niño summer. On the other hand, the El Niño was a minor one and the SST anomaly was not particularly strong. It appears that there should be other unknown mechanisms that were responsible for the unusual phenomena in the western North Pacific during the summer of 2004.

An unconventional analysis procedure was carried out in this study to contrast the variance with and without TCs. The estimated variance

difference is not likely to be the real contribution from TCs, but can probably be viewed as a quick estimation of the TCs' contribution to the ISV. The results shown above indicate that the contribution of TCs has to be taken into account to correctly estimate and interpret the ISV, especially during those years when TCs are strongly clustered by the ISO. Traditional wisdom usually assumes that the fluctuations on a shorter-time scale can be removed by time averaging or low-pass filtering. This may be true when the fluctuations in the positive and the negative phase are symmetric in both amplitude and recurrent frequency. Such a practice may be problematic for the intraseasonal variability analysis in the tropical western North Pacific, where TCs are the strongest cyclonic vortices and may not be canceled out by much weaker anticyclonic vortices. It is likely that the occurrence of TCs leaves footprints in the intraseasonal variability through the clustering effect.

The procedure adopted in this study has been used by the TC simulation and prediction community to remove the inadequate representation of TCs in the global analysis and plant an idealized vortex to represent TCs in the model. On the other hand, it is also true that TC circulation, although underestimated and sometimes unrealistic, does exist in the global analysis. It is this TC-like component that this study would like to evaluate its possible contribution to the large-scale climate variability, such as those on the intraseasonal time scale. Although the TC circulation is likely underestimated in the global analysis, the results presented above indicate that this inadequately represented TC component already contributes a significant amount of intraseasonal variability. If the TCs are accurately resolved in the global analysis, its contribution will likely be even more significant. This information will be valuable for the intraseasonal variability study, and perhaps even for the climate variability study on other time scales, as shown by Hsu *et al.* (2008).

In the tropical western North Pacific, the tropical cyclone often has a life span longer than

10 days. As the moving tropical cyclones have a strong and long-lasting energy source, large-scale circulations are likely to be induced, followed by energy emanation to remote regions. This feedback may affect the environmental flow, such as the subtropical anticyclone and monsoon trough, and leave notable footprints in the intraseasonal variability in the regions away from TC tracks. This potential effect cannot be estimated by the methodology adopted in the present study and will be explored in future works. Another problem is the coarse resolution of the datasets used in this study. Although the TCs are reasonably represented in the global analysis in the qualitative sense, the strength of the TCs is underestimated and the spatial structure is not as sharp as in the real world. As a result, the actual contribution of TCs to the ISV cannot be accurately estimated. Moreover, the contribution reported in this study is probably underestimated. Despite not being able to exactly quantify the effect, this research explains in a qualitative sense why the contribution from TCs cannot be overlooked.

Most of the general circulation models used to simulate past climate suffers from the poor simulation of the climate variability in the tropical western North Pacific during the boreal summer (Wang *et al.*, 2004). The results reported here imply that the inability to resolve and simulate TCs may be one of the key weaknesses of the GCM leading to poor simulation. Using the coarse-resolution GCM may lead to inaccurate climate simulation and prediction on the intraseasonal, interannual, and perhaps even climate change time scales. High-resolution models that are able to reasonably simulate the ensemble effect of TCs, at least in the statistical sense, seem necessary for resolving the multiscale interaction and producing better simulations of the ISV in TC-prone regions, such as the tropical western North Pacific. Although this study does not reveal any mechanism relating to the TC-ISO interaction (if there is one), it seems to imply the following. For numerical models that cannot explicitly simulate TCs in

the tropical western North Pacific, the simulated ISV is probably underestimated. Whether an improved TC simulation would improve the ISO simulation in models is an interesting issue for further study. Another implication is that the clustering effect and the TC contribution to the ISV imply a possible two-way interaction between the TC and the ISO in the tropical western North Pacific. Well-designed numerical experiments and theory development are needed to quantify and understand this process.

Our finding also raises a question about the definition of the ISV in the TC-prone regions. Traditionally, the ISV is interpreted as the variability of intraseasonally filtered perturbations. Our results, however, point out that these intraseasonal perturbations may contain the contribution from TCs, which fluctuate in much shorter periods and on a smaller spatial scale. In a region such as the tropical western North Pacific, where the mesosynoptic-scale and large-scale systems are closely intertwined, and the multiscale interaction is likely one of the key processes affecting the climate variability, the contribution from severe weather systems like TCs has to be taken into account in order to understand the mechanisms leading to the intraseasonal (and climate) variability. The present results suggest that the TC and the ISO be viewed as an integrated system to improve our understanding of the intraseasonal variability in the tropical western North Pacific.

Acknowledgements

This study was jointly supported by the Central Weather Bureau and the Nation Science Council, Taiwan, under Grant MOTC-CWB-94-6M-03 and NSC 93-2111-M-002-004-AP4, respectively.

[Received 20 September 2007; Revised 24 January 2008; Accepted 25 January 2008.]

References

- Bosilovich, M. G., and W.-Y. Sun, 1998: Monthly simulation of surface layer fluxes and soil properties during FIFE. *J. Atmos. Sci.*, **55**, 1170–1184.
- Bosilovich, M. G., and W.-Y. Sun, 1999: Numerical simulation of the 1993 Midwestern flood: land–atmosphere interactions. *J. Climate*, **12**, 1490–1505.
- Chen, T. C., S. Y. Wang, M.-C. Yen, and W. A. Gallus Jr., 2004: Role of the monsoon gyre in the interannual variation of tropical cyclone formation over the western North Pacific. *Weather and Forecasting*, **19**, 776–785.
- Elsberry, R. L., 2004: Monsoon-related tropical cyclones in East Asia. In *East Asian Monsoon* (ed. C.-P. Chang), *World Scientific Series on Meteorology of East Asia*, Vol. 2, World Scientific, Singapore, pp. 463–498.
- Gray, W. M., 1979: Hurricanes: their formation, structure and likely role in the tropical circulation. In *Meteorology over the Tropical Oceans*, D. B. Show (ed.), Royal Meteorological Society, pp. 155–218.
- Harr, P. A., and R. L. Elsberry, 1998: Large-scale circulation variability over the tropical western North Pacific. Part I: Spatial patterns and tropical cyclone characteristics. *Mon. Wea. Rev.*, **123**, 1225–1246.
- Heta, Y., 1990: An analysis of tropical wind fields in relation to typhoon formation over the Western Pacific. *J. Meteor. Soc. Japan*, **68**, 65–76.
- Hsu, H.-H., Y.-L. Chen, and W. S. Kau, 2001: Effects of ocean–atmosphere interaction on the winter temperature in Taiwan and East Asia. *Climate Dynamics*, **17**, 305–316.
- Hsu, H.-H., Y.-C. Yu, W.-S. Kau, W.-R. Hsu, W.-Y. Sun, and C.-H. Tsou, 2004: Simulation of the 1998 East Asian summer monsoon using Purdue regional model. *J. Meteor. Soc. Japan*, **82**, 1715–1733.
- Hsu, H.-H., 2005: East Asian monsoon. In *Intraseasonal Variability in the Atmosphere–Ocean Climate System*, W. K. M. Lau and D. E. Waliser (eds.), Praxis, Springer, Berlin, Heidelberg, pp. 63–94.
- Hsu, H.-H., C.-H. Hung, A.-K. Lo, C.-W. Hung, and C.-C. Wu, 2008: Influence of tropical cyclone on the estimation of climate variability in the tropical Western North Pacific. *J. Climate* (in press).

- Hsu, W.-R., and W.-Y. Sun, 1994: A numerical study of a low-level jet and its accompanying secondary circulation in a Mei-Yu system. *Mon. Wea. Rev.*, **122**, 324–340.
- Kaylor, R. E., 1977: Filtering and decimation of digital time series. Tech. Note BN 850, Institute of Physical Science Technology, University of Maryland, College Park, 42 pp.
- Kurihara, Y., M. A. Bender, and R. J. Ross, 1993: An initialization scheme of hurricane models by vortex specification. *Mon. Wea. Rev.*, **121**, 2030–2045.
- Kurihara, Y., M. A. Bender, R. E. Tuleya, and R. J. Ross, 1995: Improvements in the GFDL hurricane prediction system. *Mon. Wea. Rev.*, **123**, 2791–2801.
- Lau, K.-M., and P. H. Chan, 1986: Aspects of the 40–50-day oscillation during the northern summer as inferred from outgoing longwave radiation. *Mon. Wea. Rev.*, **114**, 1354–1367.
- Liebmann, B., H. H. Hendon, and J. D. Glick, 1994: The relationship between tropical cyclones of the Western Pacific and Indian Ocean and the Madden–Julian oscillation. *J. Meteor. Soc. Japan*, **72**, 401–412.
- Lorenc, A. C., 1984: The evolution of planetary scale 200-mb divergences during the FGGE year. *Quart. J. R. Meteor. Soc.*, **110**, 427–441.
- Maloney, E. D., and M. J. Dickinson, 2003: The intraseasonal oscillation and the energetics of summertime tropical Western North Pacific synoptic-scale disturbances. *J. Atmos. Sci.*, **60**, 2153–2168.
- McBride, J. L., 1995: Tropical cyclone formation. In Chap. 3, *Global Perspectives on Tropical Cyclones*. Tech. Doc. WMO/TD No. 693, World Meteorological Organization, Geneva, Switzerland, pp. 63–105.
- Nakazawa, T., 1986: Intraseasonal variations of OLR in the tropics during the FGGE year. *J. Meteor. Soc. Japan*, **64**, 17–34.
- Nakazawa, T., 2006: Madden–Julian oscillation activity and typhoon landfall on Japan in 2004. *SOLA*, **2**, 136–139, doi:10.2151/sola.2006-035.
- Sun, W.-Y., J.-D. Chern, C.-C. Wu, and W. R. Hsu, 1991: Numerical simulation of mesoscale circulation in Taiwan and surrounding area. *Mon. Wea. Rev.*, **119**, 2558–2573.
- Sun, W.-Y., and J.-D. Chern, 1993: Diurnal variation of lee vortices in Taiwan and surrounding area. *J. Atmos. Sci.*, **51**, 191–209.
- Sun, W. Y., J. D. Chern, and M. Bosilovich, 2004: Numerical study of the 1988 drought in the United States. *J. Meteorol. Soc. Japan*, **82**, 1667–1678.
- Torrence, C., and G. P. Compo, 1998: A practical guide to wavelet analysis. *Bull. Amer. Meteor. Soc.*, **79**, 61–78.
- Wang, B., and H. Rui, 1990: Synoptic climatology of transient tropical intraseasonal convection anomalies: 1975–1985. *Meteor. Atmos. Phys.*, **44**, 43–61.
- Wu, C.-C., T.-H. Yen, Y.-H. Kuo, and W. Wang, 2002: Rainfall simulation associated with Typhoon Herb (1996) near Taiwan. Part I: The topographic effect. *Wea. Forecasting*, **17**, 1001–1015.